Pressure Effect on the Chain Shrinkage of Poly(vinylpyrrolidone) Induced by Complexation with a Hydrophobic Compound in Aqueous Solution

Naoki Tanaka,*,† Motoyoshi Takemura,† Takashi Konno,‡ and Shigeru Kunugi†

Laboratory for Biopolymer Physics, Department of Polymer Science and Engineering, Kyoto Institute of Technology, Sakyo, Kyoto, 606-8585, Japan, and National Institute for Physiological Science, Myodaiji, Okazaki 444-8585, Japan

Received February 25, 1998; Revised Manuscript Received September 22, 1998

ABSTRACT: The effects of pressure on the binding of a hydrophobic compound (8-anilino-1-naphthalenesulfonate (ANS)) to poly(vinylpyrrolidone) (PVP) in aqueous solution were followed by the fluorescence enhancement over the pressure range 0.1−400 MPa. An elevation in pressure induced the dissociation of ANS from an oligomer PVP (molecular weight <6000) but favored its binding to a larger PVP molecule (MW > 10 000). We calculated the binding constant between ANS and PVP (K_b) and estimated the apparent volume changes accompanying the ANS binding to PVP (ΔV_b) from the pressure dependence of K_b. The volume changes for ANS binding to high-MW PVP's were dependent on the pressure, and negative values were obtained in the pressure region from 100 to 400 MPa. SAXS measurements demonstrated that the ANS binding to the high-MW PVP chain led to the reduction of radii of gyration, suggesting that ANS binding induced local cluster formation in the PVP chain around the binding site. The Kratky plot indicated that global shrinkage of the chain occurred, and the negative volume change for ANS binding to high-MW PVP is explained by the fact that the cluster formation around the ANS is followed by an inclusion of the cluster around ANS into the random coil for PVP.

Introduction

The properties of a water solution of poly(*N*-vinyl-2-pyrrolidone) (PVP) have been extensively studied.[1−8] PVP interacts with various small molecules, and many studies have been done to elucidate the mechanism of the interaction between synthetic polymer with low molecular compounds. It has been shown that the coil dimensions of PVP are reduced when it forms a complex with hydrophobic molecules[1−3] and hydrophobic interaction is the dominant force in the complex. Application of high pressure yields unique information concerning the physical property of the interactions, and many studies using high pressure have been done for synthetic polymers[9−11] and protein structures.[12−18] In the present study, we investigated the effect of pressure on the binding of a hydrophobic compound to PVP. When the fluorescence dye 8-anilino-1-naphthalenesulfonate (ANS) is used as a probe, its binding to PVP leads to an increase in fluorescence that is proportional to the number of bound ANS. We have followed the ANS binding at elevated pressures and calculated apparent binding constants between ANS and various molecular weights of PVP at elevated pressure. The solution X-ray scattering experiments were performed to observe the changes of the dimension and the overall shape of PVP chain induced by ANS binding. We elucidated a mechanism for the interaction between PVP and ANS by using these experimantal results.

Materials and Methods

Materials. PVP samples with molecular weights of 55 000 (PVP 55K) and 1 300 000 (PVP 1300K) were purchased from Aldrich (Milwaukee, WI) and purified by dialysis. PVP was fractionated using Sephadex gel G-100 (Pharmacia Biotech, Uppsala, Sweden). The molecular weight of the fractions was determined by GPC. Fractions with a weight-average molecular weights of 10 000 (PVP 10K) and 2000 (PVP 2K), as well as PVP 55K and PVP 1300K, were used in this study. The water for the sample solutions was purified using a Barnstead E-pure system (Barnstead Thermolyne Co., Iowa City, IA).

Methods. The fluorescence titration of PVP (2 mg/L) with ANS at elevated pressures was performed using high-pressure cells possessing three optical windows manufactured by Teramecs Co. (Kyoto, Japan), combined with a Shimadzu RF5000 spectrofluorimeter (Kyoto, Japan) at 25 °C. The concentration of ANS was determined using a molar absorbance coefficient of 6300. When an excitation wavelength of 410 nm was used, the fluorescence intensity of the free ANS was negligible compared with fluorescence intensity of ANS bound to PVP. Thus, the fluorescence intensity of ANS is proportional to the concentration of bound ANS under this excitation condition. The emission intensity at 480 nm (I_{obs}) was measured over a pressure range from 0.1 to 400 MPa. The fluorescence intensity I_{obs} was corrected for the inner filter effect as follows:

$$I_{cor} = I_{obs} \times 10^{(A_{ex} + A_{em})/2} \quad (1)$$

where I_{cor} is the corrected fluorescence intensity at 480 nm, and A_{ex} and A_{em} are the absorbance values of the sample solution in a high-pressure cell (diameter 1.0 cm) at excitation and emission wavelengths, respectively. We obtained I_{cor} values for 1 μM ANS in the presence of an excess concentration of PVP, in which all ANS molecules are bound to PVP, over a pressure range from 0.1 to 400 MPa. These values were used as the standard for the calculation of the concentration of ANS bound to PVP at each point of the titration at each pressure. The concentrations of ANS and PVP at elevated pressures were also corrected using the values for the specific volume of water.[19]

For the analysis of the ANS binding data, a Klotz analysis[20] was initially performed using the number of moles of ANS bound per base mole of pyrrolidone residues. A more sophisticated stoichiometric analysis of the data is described in the

* To whom correspondence should be addressed. Tel +81-75-724-7861, FAX +81-75-724-7710 e-mail tanaka@ipc.kit.ac.jp.
† Kyoto Institute of Technology.
‡ National Institute for Physiological Science.

10.1021/ma980289t CCC: $15.00
Published on Web 11/12/1998

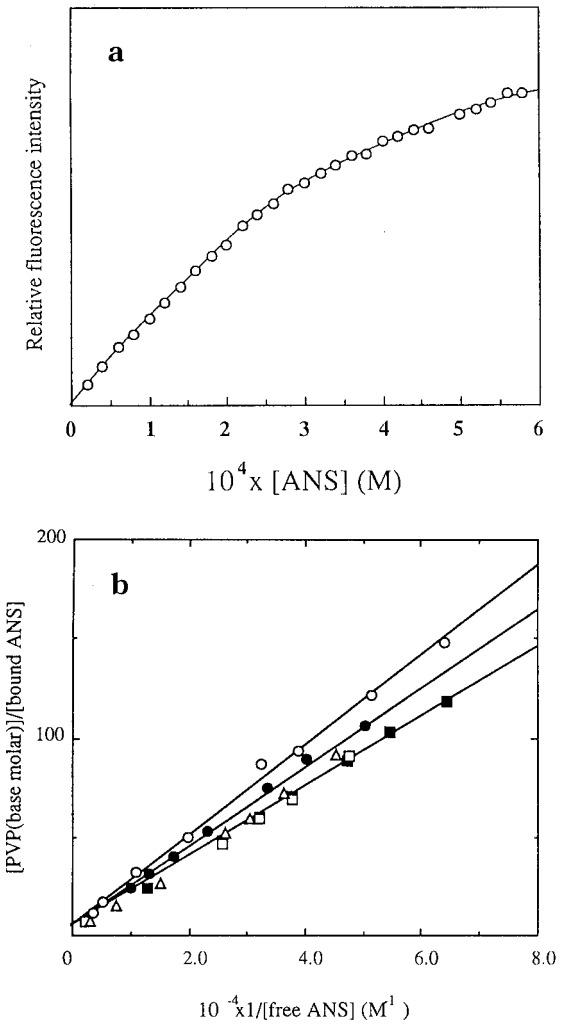

Figure 1. (a) Fluorescence titration of PVP 2K with ANS. (b) Klotz plots for the titration of ANS with various molecular weights of PVP: ○, PVP 2K; ●, PVP 6K; □, PVP 10K; ■, PVP 55K; △, PVP 1300K.

Table 1. Apparent K_b Values (L/Base mole) for the Binding between PVP and ANS at 0.1 MPa Deduced from the Klotz Plot Analysis

PVP	2K	6K	10K	55K	1300K
K_b	4461.3	4842.4	5569.8	5727.4	5975.9

Discussion. The data fitting by this model (eq 3 in the Discussion) was performed using a nonlinear least-squares program (Levenberg−Marquardt algorithm) run on a Power Macintosh computer (Apple). This fitting procedure was applied to 30−50 data points, with two independent variables and two fitting free parameters. The solution X-ray scattering experiments on PVP were carried out with a solution scattering station (SAXS camera) installed at BL-10C, the Photon Factory, Tsukuba, Japan.[21,22] The sample-to-detector distance was about 90 cm for the SAXS measurements, calibrated with the meridional diffraction of dried chicken collagen. The wavelength of the X-ray was 1.488 Å. The sample cell thermostated to 25 °C had a volume of 50 μL with 15 μm thick quartz windows and had a 1 mm X-ray path length. The PVP concentration was varied from 3 to 10 mg/mL, and the measurement time for each scattering experiment was 10 min. Scattering from a solution containing no PVP was measured in order to subtract background scattering from that of the PVP-containing solutions. Data processing was carried out with a Macintosh (Apple) personal computer. X-ray scattering intensities at the small-angle region are given as $I(Q) = I(0) \exp(-R_g^2Q^2/3)$, where Q and $I(0)$ are the momentum transfer and the intensity at 0 scattering angle, respectively. Q is defined by $Q = 4\pi \sin\theta/\lambda$ (in Å^{-1}), where 2θ and λ are the scattering angle and the wavelength of the X-ray, respectively. The radius of gyration (R_g) was obtained from the slope of the Guinier plot, a plot of $\ln[I(Q)]$ against Q^2.

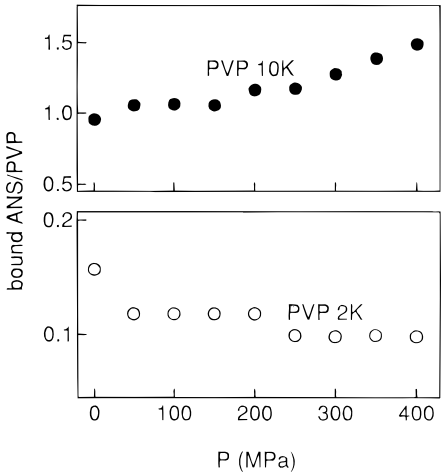

Figure 2. Average number of ANS molecules bound to a PVP molecule as a function of the pressure P: ○, PVP 2K ([ANS] = 19.6 μM at 0.1 MPa); ●, PVP 10K ([ANS] = 21.3 μM at 0.1 MPa).

Results

Fluorescence Titration of PVP with ANS under Ambient Pressure. The binding of ANS to PVP of various molecular weights was monitored quantitatively by a fluorescence titration method. The fluorescence intensity of ANS is enhanced when it forms a complex with PVP in aqueous solution[1] because of the apolar microenvironment of the binding site.[23,24] Thus, the fluorescence change in the titration of PVP with ANS is proportional to the concentration of ANS bound to PVP. Figure 1a shows the results of the ANS titration of the PVP 10K solution monitored by the fluorescence intensity. Using this simple-binding assumption, the data were analyzed by the Klotz plot:

$$\frac{1}{r} = \frac{1}{nK_b}\frac{1}{a} + \frac{1}{n} \qquad (2)$$

where r is the number of ANS molecule bound to PVP per base mole of pyrrolidone residue, a is the concentration of free ANS, K_b is the binding constant, and n is number of ANS molecule binding sites on the PVP (per base mole of pyrrolidone residues). The $1/n$ value, the number of pyrrolidone residues required to form an ANS binding site, is obtained from the y-intercept, and the K_b value is determined from the inverse of slope of the plots and the y-intercept. As shown in Figure 1b, the Klotz plots for most PVP samples were linear, thus indicating that the binding of ANS to PVP was noncooperative. The $1/n$ values for all of the PVP samples fell into almost the same range (a $1/n$ value of about 10), indicating that a ANS molecule binds to a unit composed of 10 pyrrolidone residues in the polymer chain, similar to result obtained for the binding of other aromatic molecules.[25] Table 1 lists K_b values obtained for different PVP.

Fluorescence Titration of PVP with ANS under Elevated Pressure. The ANS titration experiments were carried out over a pressure range from 0.1 to 400 MPa. Figure 2 shows two plots of the average number of ANS molecules bound to a PVP molecule as a function

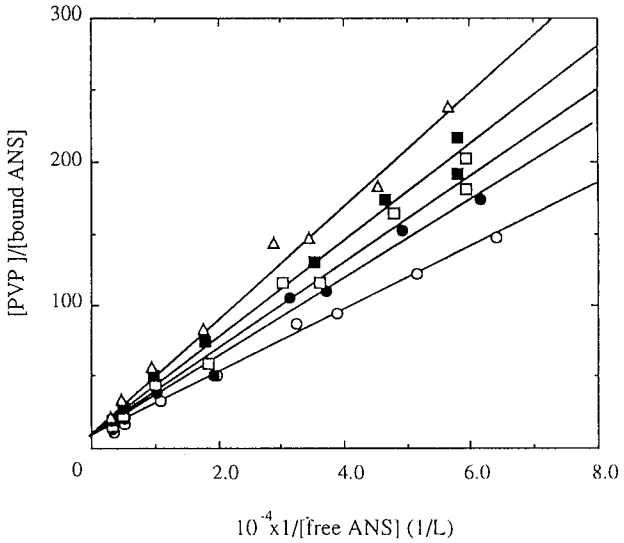

Figure 3. Klotz plots for the ANS titration using PVP 2K under various pressures: ○, 0.1 MPa; ●, 100 MPa; □, 200 MPa; ■, 300 MPa; △, 400 MPa.

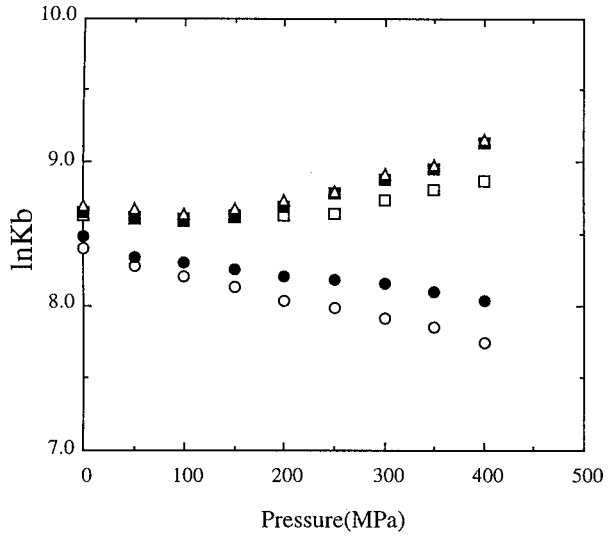

Figure 4. Plots of ln K_b against the pressure P for various PVP samples. The apparent ANS binding constant K_b was estimated from the slope of the Klotz plots, such as those in Figure 3. ○, 2K; ●, 6K; □, 10K; ■, 55K; △, 1300K.

of pressure. A comparison of the plots for PVP 2K ([ANS] = 19.6 μM) with PVP 10K ([ANS] = 21.3 μM) shows that whereas ANS binding to PVP 2K was suppressed by an increase in pressure, the binding to PVP 10K was enhanced. Klotz analyses were performed for each PVP sample to yield estimates of the apparent K_b and n at various pressures (Figure 3 for PVP 2K). The n value, i.e., the number of ANS binding sites on PVP, was independent of pressure. It is striking that the K_b for PVP 2K and 6K decreased with increasing pressure, whereas the high-MW PVP (MW > 10K) showed the opposite tendency (Figure 4).

Small-Angle X-ray Scattering of PVP10K Solutions. We performed small-angle X-ray scattering analysis (SAXS) to observe the changes in the dimensions of PVP induced by ANS binding. Guinier plots of the SAXS data yield estimates for the radius of gyration (R_g), related to the size of the chain molecule. Figure 5a shows the Guinier plots of PVP 10K in the presence (stars) and absence (open circles) of 10 mM ANS. These scattering curves for infinite dilution were obtained by

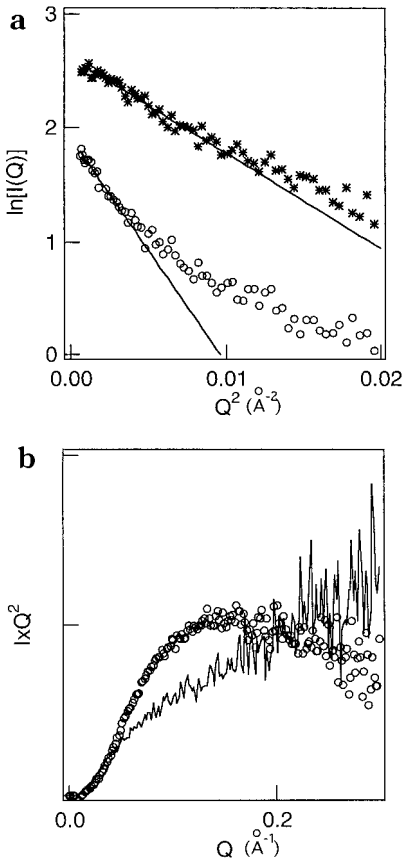

Figure 5. (a) Guinier plots of PVP 10K at pH 7.0 in the presence (star) and absence (open circle) of 10 mM ANS. The scattering curves for infinite dilution were obtained by extrapolating the scattering data at 3, 5, 8, and 10 mg/mL of PVP for all of these measurements. The ratio of ANS to monomer residues was over 10:1. Both plots have linear regions in the low Q range (Guinier region; defined as R_gQ < 1.3 here), and the radii of gyration were estimated by linearly fitting of data points in these regions. (b) Kratky plots of 10 mg/mL PVP 10K in the presence (open circle) and absence (solid line) of 10 mM ANS.

extrapolating the scattering data at 3, 5, 8, and 10 mg/mL PVP. Both plots in Figure 5a are linear in the low Q range (Guinier region), and the radii of gyration were estimated by linearly fitting the data points in this region. Note that we chose the Guinier regions by a criteria of R_gQ < 1.3 in the present study.[22,26] The R_g values of PVP 10K in the presence and absence of ANS were estimated to be 15.8 ± 0.7 and 24.4 ± 1.1 Å, respectively. The results clearly showed that the binding of ANS to PVP 10 K drastically reduced the expansion of the chain molecule.

The Kratky plot of $I(Q)Q^2$ versus Q plot is useful in describing the overall shape of the polymer chain molecule.[22,26,27] In essence, the Kratky plot shows a clear peak for a globular conformation but has a plateau shape and then increases monotonically for a flexible chainlike molecule. Figure 5b shows the Kratky pattern for PVP 10K at 10 mg/mL in the presence (open circles) and absence (solid line) of 10 mM ANS. In the absence of ANS, the monotonically increasing Kratky pattern indicates that the PVP chain was in a flexible chainlike conformation. The addition of ANS drastically changed the Kratky pattern for PVPs, and the plot in this case increases sharply in the low Q range and exhibits a maximum at Q = 1.7 Å^{-1}, corresponding to a globular shape for the PVP chain. The results from the Kratky

Table 2. ΔV Values for the Binding between PVP and ANS

PVP pressure region[a]	2K	6K	10K low	10K high	55K low	55K high	1300K low	1300K high
ΔV (mL/mol)	+3.5	+2.4	+0.9	−1.6	+0.9	−4.9	+1.0	−4.9

[a] Low-pressure region, <100 MPa; high-pressure region, from 100 to 400 MPa.

plot, together with the estimates of R_g, demonstrated that the PVP molecule in water has a highly expanded flexible chain conformation but has a restricted spatial distribution and a globular shape in the presence of ANS. The binding of ANS to PVP induced the shrinkage of PVP 10K, probably because of the high affinity of ANS to the hydrophobic core of the shrunken form of the PVP chain.

Discussion

The SAXS data in Figures 5 showed that the binding of ANS to the high-MW PVP was strongly coupled with a shrinkage of the chain molecule. Klotz plots of ANS binding to PVP were linear (Figure 1b), indicating that the PVP chain shrinks gradually as more ANS binds to the polymer chain. These results suggest that ANS binding induces local cluster formation in the PVP chain around the binding site. The Klotz analysis of ANS binding to PVP at ambient pressure in Figure 1b shows that different high-MW PVP's (>10 K) had similar K_b values, but the K_b's for low-MW PVP's (<6 K) were smaller than these values. PVP 2K is composed of about 20 pyrrolidone residues, which is in the same range as a unit in the polymer chain for ANS binding (10 pyrrolidone residues). This means that the K_b value for PVP 2K almost corresponds to that for binding between ANS and a unit in the polymer chain for ANS molecule binding. Therefore, higher K_b values of high-MW PVP may be due to the fact that the cluster around the ANS is followed by an inclusion of the cluster into the random coil for the high-MW PVP. The SAXS data in Figures 5b indicate that PVP chain has a globular shape when it binds to ANS. This result suggests that a global conformational change occurs for high-MW PVP, and this is consistent with the model above.

The apparent change in volume upon ANS binding to PVP (ΔV_b) is obtained from the slope of ln K_b against pressure (Figure 4) using the following equation

$$\Delta V_b = \frac{-RT \, \mathrm{d} \ln K_b}{\mathrm{d}P} \tag{3}$$

and is summarized in Table 2. The plot of K_b against pressure for high-MW PVP was not linear, and we therefore estimated ΔV_b values from the linear regions of the plots in low-pressure (<100 MPa) and in high-pressure (from 100 to 400 MPa) regions, respectively. Torgerson et al. obtained ΔV_b values for ANS binding to poly-β-cyclodextrin of +9.3 mL/mol[2]. They explained that the ΔV_b value was positive because the ANS binding site of poly-β-cyclodextrin was incompressible compared to the case of water. The value determined here for PVP 2K, $\Delta V_b = +3.5$ mL/mol, is consistent with their results and suggests that the parts of PVP involved directly in the ANS binding site are also incompressible in comparison with water. The larger ΔV value for poly-β-cyclodextrin than for PVP was probably due to the specific structural properties of the ANS binding site of poly-β-cyclodextrin, which is composed of a covalently bonded ring of sugar residues. A large number of water molecules must be eliminated from the ring of β-cyclodextrin when ANS binds to poly-β-cyclodextrin.

Negative values were obtained for apparent ΔV_b's for high-MW PVP in the high-pressure region. Assuming that the volume change for the binding of ANS to high-MW PVP itself is comparable to PVP 2K, an inclusion of the cluster around ANS into the random coil has remarkable negative contribution for apparent ΔV_b in high-pressure region. It has generally been accepted that the PVP molecule contained both hydrogen bond donors are hydrophobic interactions.[6] The question arises as to what type of physical interactions was most responsible for the negative volume change during the inclusion of the cluster. Sun and King, in their study of the aggregation processes of PVP, have claimed that the formation of highly directional hydrogen bonds increase the volume of the system, whereas hydrophobic interactions tend to decrease the volume under high pressure.[6] Their opinion on these hydrophobic interactions was probably based on the negative ΔV_b for the transfer of a small nonpolar molecule from an aqueous to a liquid hydrocarbon environment under relatively high pressure (>100 MPa).[29] Following this line of thinking, an inclusion of the cluster around ANS into the random coil for the high-MW PVP may be driven by hydrophobic interactions, which seems to be physically reasonable since the ANS-bound PVP has a large number of hydrophobic residues. The present results are useful for the elucidation of the mechanisms of the interaction of PVP with small molecules in aqueous solution. In further studies, we will investigate the interaction of various PVP derivatives with low molecular compounds under high pressure.

Acknowledgment. The X-ray scattering measurements were performed with an approval from the Program Advisory Committee of the Photon Factory (Proposal No. 95G-262). We are indebted to Dr. M. Kataoka for his support with experiments at the Photon Factory.

References and Notes

(1) Kirsh, Y. E.; Soos, T. A.; Karaputadze, T. M. *Eur. Polym. J.* **1979**, *15*, 223−228.
(2) Klech, C. M.; Cato III, A. E.; Suttle III, A. B. *Colloid Polym. Sci.* **1991**, *269*, 643−649.
(3) Gargallo, L.; Radic, D. *Polymer* **1983**, *24*, 91−94.
(4) Takagishi, T.; Hosokawa, T.; Hatanaka, Y. *J. Polym. Sci. Part A: Polym. Chem.* **1989**, *27*, 1−13.
(5) Takagishi, T.; Hosokawa, T. *Polym. Sci., Part A: Polym. Chem.* **1989**, *27*, 1925−1933.
(6) Sun, T.; King, Jr., H. E. *Macromolecules* **1996**, *29*, 3175−3181.
(7) Sun, T.; King, Jr., H. E. *Phys. Rev. E* **1996**, *54*, 2696−2703.
(8) Tanaka, N.; Kitano, H. *Macromol. Chem. Phys.* **1994**, *195*, 3369−3380.
(9) Kunugi, S.; Takano, K.; Tanaka, N.; Suwa, K.; Akashi, M. *Macromolecules* **1997**, *30*, 4499−4501.
(10) Suwa, K.; Yamamoto, K.; Akashi, M.; Takano, K.; Tanaka, N.; Kunugi, S. *Colloid Polym. Sci.* **1998**, *276*, 529−533.
(11) Kunugi, S.; Takano, K.; Tanaka, N.; Akashi, M. *Proceeding of the 35th EHPRG Meeting*; The Royal Society of Chemistry: London, United Kingdom, 1998; pp 61−66.
(12) Kauzmann, W. *Nature* **1987**, *325*, 763−764.
(13) Heremans, K. *Annu. Rev. Biophys. Bioeng.* **1982**, *11*, 1−21.
(14) Weber, G.; Drickamer, H. *Q. Rev. Biophys.* **1983**, *16*, 89−112.
(15) Jonas, J.; Jonas, A. *Annu. Rev. Biophys. Biomol. Struct.* **1994**, *23*, 287−318.

(16) Tanaka, N.; Nakajima, K.; Kunugi, S. *Int. J. Peptide Protein Res.* **1996**, *48*, 259−264.

(17) Tanaka, N.; Nishizawa, H.; Kunugi, S. *Biochim. Biophys. Acta* **1997**, *1338*, 13−20.

(18) Tanaka, N.; Tonai, T.; Kunugi, S. *Biochim. Biophys. Acta* **1997**, *1339*, 226−232.

(19) Sato, H.; Uematsu, M.; Watanabe, K.; Saul, A.; Wagner, W. *J. Phys. Chem. Ref. Data* **1988**, *17*, 1439−1540.

(20) Klotz, I. M.; Walker, F. M.; Pivan, R. B. *J. Am. Chem. Soc.* **1946**, *68*, 1486−1490.

(21) Ueki, T.; Hiragi, Y.; Kataoka, M.; Inoko, Y.; Tagawa, H.; Muroga, Y. *Biophys. Chem.* **1985**, *23*, 115−124.

(22) Konno, T.; Kataoka, M.; Kamatari, Y.; Kanaori, K.; Nosaka, A.; Akasaka, K. *J. Mol. Biol.* **1995**, *251*, 95−103.

(23) Wang, Y.; Morawetz, H. *Macromolecules* **1986**, *19*, 1925−1930.

(24) Bednar, B.; Trnena, J.; Svoboda, P.; Vajda, S.; Fidler, V.; Prochazka, K. *Macromolecules* **1991**, *24*, 2054−2059.

(25) Molyneux, B. P.; Frank, H. P. *J. Am. Chem. Soc.* **1961**, *83*, 3169−3174.

(26) Konno, T.; Kamatari, Y.; Kataoka, M.; Akasaka, K. *Protein Sci.* **1997**, *6*, 2242−4449.

(27) Glatter, O.; Kratky, O. *Small-Angle X-ray Scattering*; Academic Press: New York, 1982.

(28) Torgerson, T.; Drickamer, H. G.; Weber, G. *Biochemistry* **1979**, *18*, 3079−3083.

(29) Sawamura, S.; Kitamura, K.; Taniguchi, Y. *J. Phys. Chem.* **1989**, *93*, 4931−4935.

MA980289T